Measuring the Dark Energy and Primordial Non-Gaussianity: Forecasts for the Tianlai Cylinder Array

Yidong Xu (NAOC), Xin Wang (JHU), Xuelei Chen (NAOC)

2015-09-08@Balikun

Xu, Wang & Chen 2015, ApJ, 798, 40

Outline

- Introduction
  - Baryon Acoustic Oscillations (BAO) and Dark Energy
  - The primordial non-Gaussianity (PNG) and its imprint on the large scale structure
  - Intensity Mapping and the Tianlai Cylinder Array
- The Power Spectrum Measurement with Tianlai Intensity Mapping
  - Signal power spectrum and noise power spectrum
- Fisher Forecast on the Constraint on Dark Energy
- Fisher Forecasts for the PNG
  - PNG from scale-dependent bias
  - PNG from bispectrum

Dark Energy and its Probes

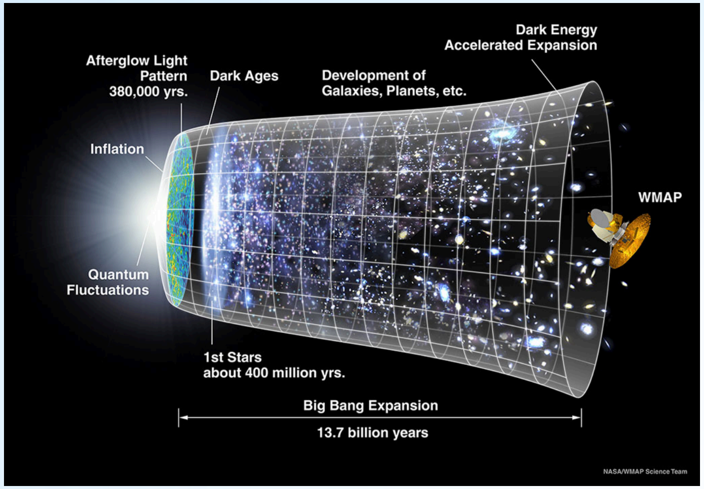

Credit: NASA / WMAP Science Team

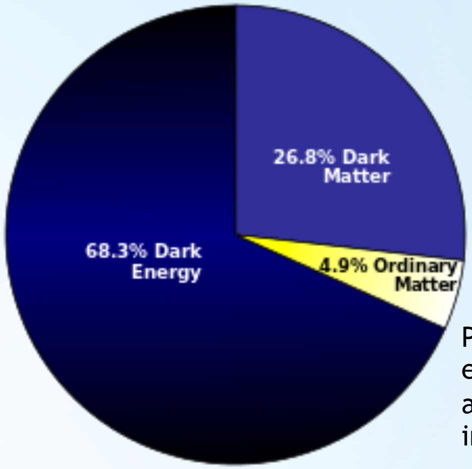

Proportion of dark energy, dark matter, and ordinary matter in the universe.

* "Seeing" the dark energy via…

- The expansion rate of the universe:

$$\frac{H(z)}{H_0} = \left[\Omega_m(1+z)^3 + \Omega_k(1+z)^2 + \Omega_X e^{3\int_0^z \frac{1+w(z')}{1+z'}dz'}\right]^{1/2}$$

- The growth rate of structures f(z) : crucial for testing extra ρ components vs modified gravity.

✓ Standard candles:

- measure d_L (integral of H^{-1})

✓ Standard rulers:

- measure d_A (integral of H^{-1}) and H(z)

Baryon Acoustic Oscillations – the cosmological standard ruler

* BAOs are the frozen sound waves that were present in the photon-baryon plasma prior to recombination.
* The standard ruler of the sound horizon at the last scattering surface
  * $r_s(z_d)$ = 153.3 ± 2.0 Mpc (Komatsu et al. 2009)

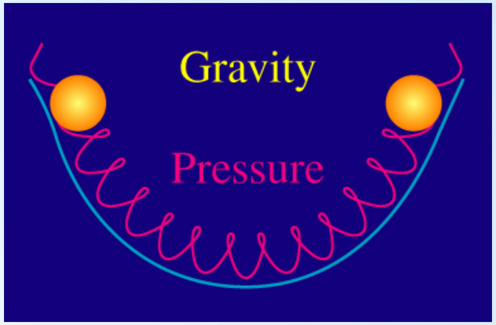

Freezed pattern

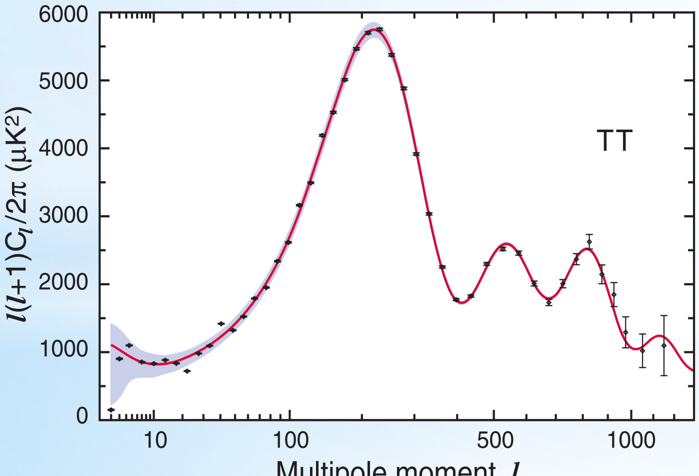

The nine-year WMAP TT angular power spectrum. (arXiv:1212.5225v3)

Statistical standard ruler

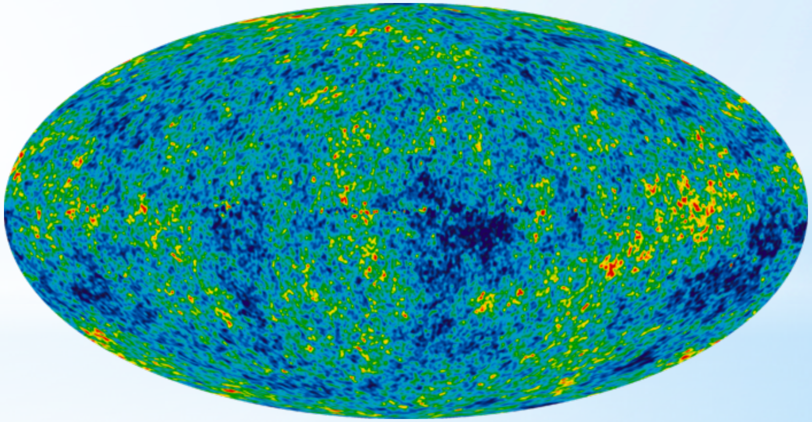

Temperature anisotropies of the CMB based on the nine year WMAP data (2012).(Credit: NASA / WMAP Science Team)

Baryon Acoustic Oscillations on large-scale structures

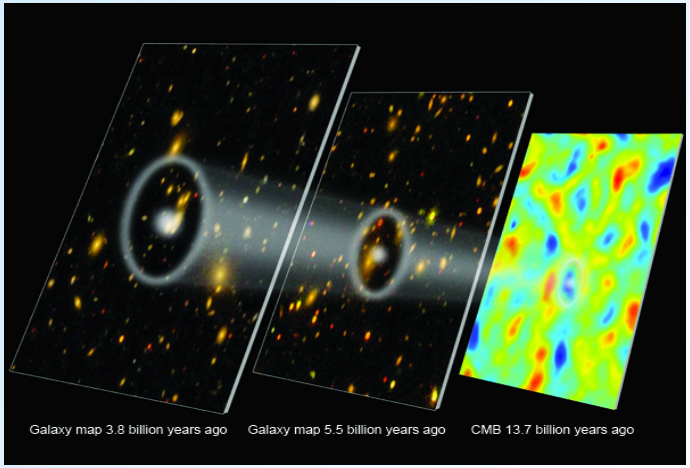

(E.M. Huff, the SDSS-III team, and the South Pole Telescope team. Graphic by Zosia Rostomian.)

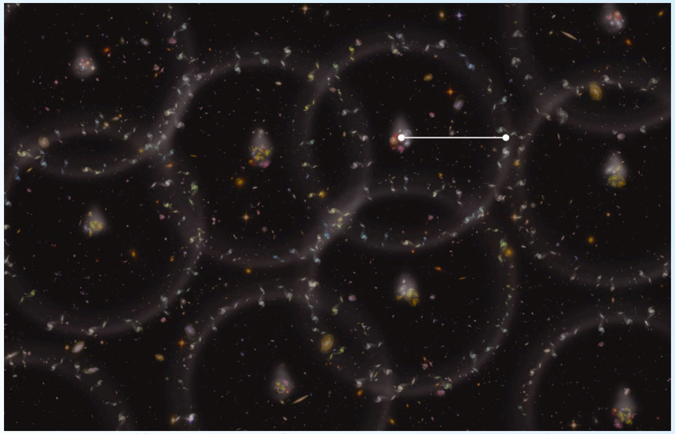

An artist's illustration depicting exaggerated BAOs in the distant universe. (Zosia Rostomian (LBNL), SDSS-III, BOSS)

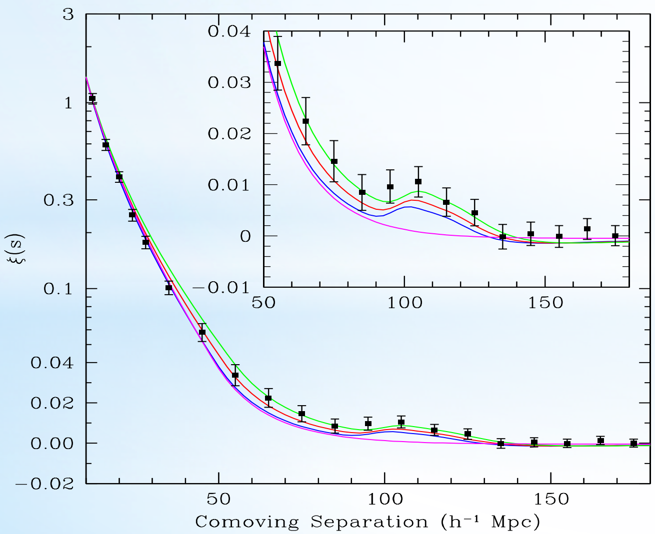

BAP in the clustering of the SDSS LRG galaxy sample (Eisenstein et al. 2005)

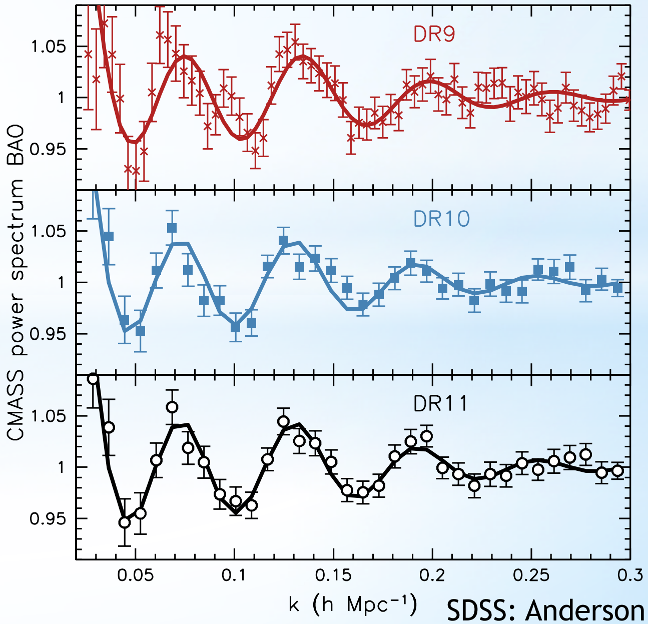

SDSS: Anderson et al. 2014

Baryon Acoustic Oscillations as a Probe of Dark Energy

* The BAOs imprint features on the CMB as well as large-scale structures (LSS) in the later universe.

➔ a standard ruler at various z to measure the angular diameter distance $D_A(z)$ and the Hubble parameter H(z)

➔ expansion rate

➔ properties of dark energy

The LSS as a Probe of the Primordial Non-Gaussianity

* Inflation → Initial density perturbations → Structure Formation → LSS today

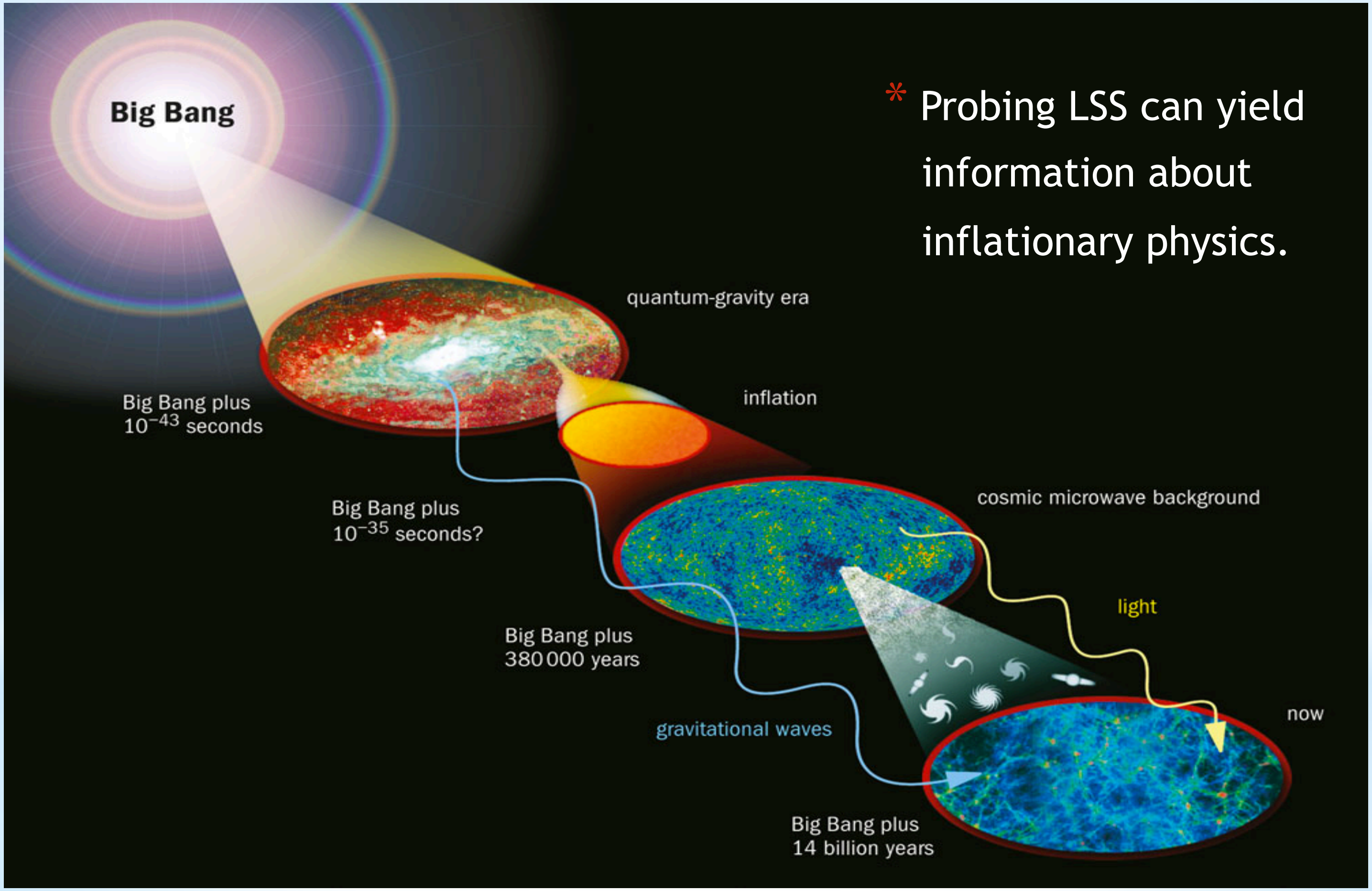

* Probing LSS can yield information about inflationary physics.

(Courtesy: NASA)

The LSS as a Probe of the Primordial Non-Gaussianity

* Standard slow-roll inflation – nearly Gaussian density fields

$$\langle \Phi(\mathbf{k})\Phi^*(\mathbf{k}')\rangle = (2\pi)^3 \delta_D(\mathbf{k}-\mathbf{k}')P_\Phi(k)$$

* Other inflation mechanisms – potentially detectable non-Gaussianity
* Lowest order non-Gaussianity: bispectrum

$$\langle \Phi(\mathbf{k}_1)\Phi(\mathbf{k}_2)\Phi(\mathbf{k}_3)\rangle = (2\pi)^3\, \delta_D(\mathbf{k}_{123})\, B_\Phi(k_1,k_2,k_3)$$

$$B_\Phi(k_1,k_2,k_3) \equiv f_{\rm NL} F(k_1,k_2,k_3)$$

amplitude | shape

(Model-dependent)

* The PNG as a powerful probe to the dynamics of inflation.

The LSS as a Probe of the Primordial Non-Gaussianity

* PNG imprint on the CMB:
  - Angular bispectrum measurement

$$\begin{pmatrix} f_{\rm NL}^{\rm loc} = 2.5 \pm 5.7 \\ f_{\rm NL}^{\rm eq} = -16 \pm 70 \\ f_{\rm NL}^{\rm orth} = -34 \pm 33 \end{pmatrix} (68\,\%\,{\rm CL}, T) \quad \begin{pmatrix} f_{\rm NL}^{\rm loc} = 0.8 \pm 5.0 \\ f_{\rm NL}^{\rm eq} = -4 \pm 43 \\ f_{\rm NL}^{\rm orth} = -26 \pm 21 \end{pmatrix} (68\,\%\,{\rm CL}, T+E)$$

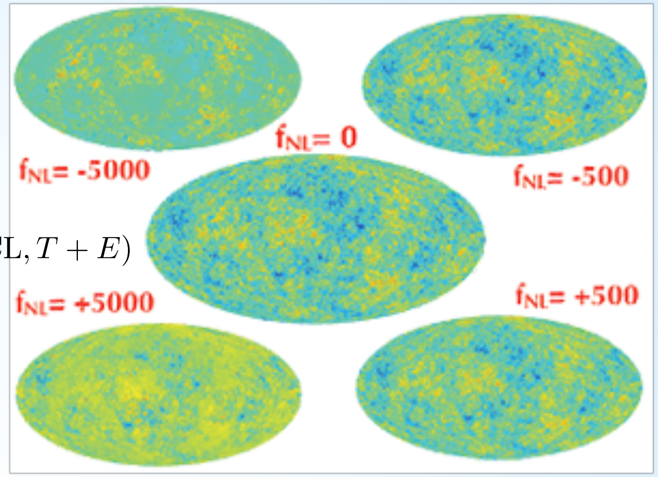

* PNG effects on LSS:
  - High-order correlations of galaxy distribution – bispectrum, trispectrum

(e.g. Sefusatti & Komatsu 2007)

  - Abundance of rare objects – cluster number density

(e.g. Afshordi & Tolley 2008; Dalal *et al*. 2008)

  - The large-scale clustering of halos – scale-dependent bias

(e.g. Dalal et al. 2008; Desjacques et al. 2011)

LSS measured in radio – HI galaxy survey

* Currently: ALFALFA
  * limited to z <~0.2
* Upcoming: FAST, ASKAP, MeerKAT
  * Higher sensitivities, but still challenging at high redshift
* Future: SKA
  * Comparable to the existing optical galaxy surveys (Rawlings et al. 2004; Abdalla et al. 2010)

HI Intensity Mapping

* The 21 cm intensity mapping technique
  * During EoR – HI gas in the IGM ➔ Post-EoR – HI gas in halos
* 21 cm cosmology with ***intensity mapping***
  * High efficiency
  * Map the large scale structure at 0 < *z* < *3*
  * Tested with the Green Bank Telescope (GBT) and the Parkes telescope

  (Chang et al. 2010; Masui et al. 2013; Switzer et al. 2013)

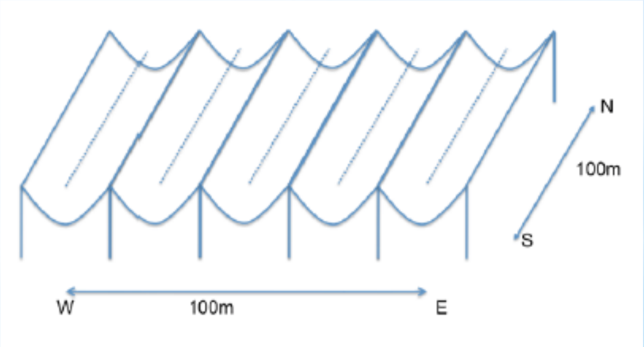

* The cylinder interferometer array design
  * Tianlai (天籁)
  * CHIME
* Competitive with Stage III dark energy experiments

  (e.g. Chang et al. 2008; Seo et al. 2010; Ansari et al. 2012)

The Tianlai cylinder array

表 1.1: The experiment parameters for Tianlai.

	cylinders	width	length	dual pol. units/cylinder	Frequency
Pathfinder	3	15 m	40 m	32	700 – 800 MHz
Pathfinder+	3	15 m	40 m	72	700 – 800 MHz
Full scale	8	15 m	120 m	256	400 – 1420 MHz

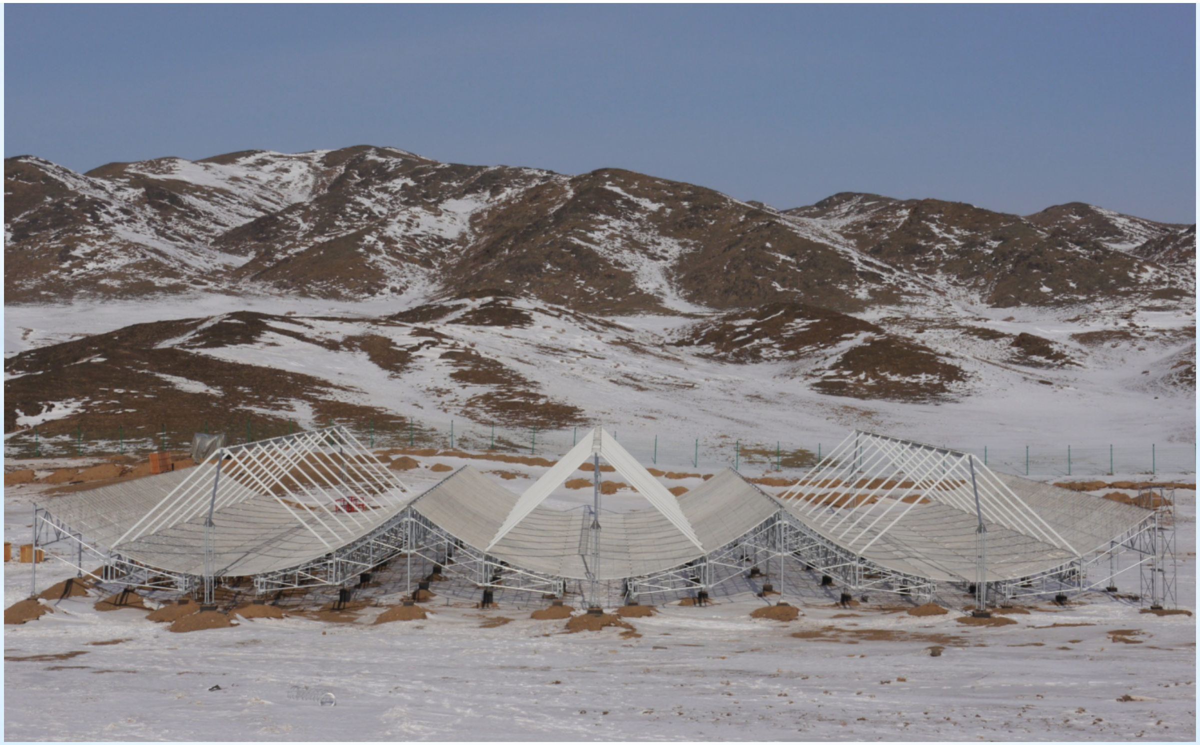

The Power Spectrum Measurement with Tianlai Intensity Mapping

* The Signal Power Spectrum

$$P_{\rm obs}(k_{{\rm ref}\perp}, k_{{\rm ref}\parallel}) = \frac{D_A(z)^2_{\rm ref} H(z)}{D_A(z)^2 H_{\rm ref}(z)} \left(b_1^{\rm H\,I}(z) + f(z) \frac{k_\parallel^2}{k_\perp^2 + k_\parallel^2} \right)^2 \times G(z)^2 P_{\rm m0}(k) + P_{\rm shot}, \quad (2)$$

$$\frac{H(z)}{H_0} = \left[\Omega_m (1+z)^3 + \Omega_k (1+z)^2 + \Omega_X e^{3 \int_0^z \frac{1+w(z')}{1+z'} dz'} \right]^{1/2}$$

and

$$D_A(z) = \frac{c}{1+z} \int_0^z \frac{dz'}{H(z')}.$$

- The linear growth rate f(z) affects the observed power spectrum

through the RSD factor β, by $\beta = f(z)/b_1^{\rm H\,I}(z)$,

and through the linear growth factor G(z) by $f = \frac{d \ln G(a)}{d \ln a} = -\frac{(1+z)}{G(z)} \frac{dG(z)}{dz}$

The Signal Power Spectrum

* The intensity mapping measures the power spectrum of brightness temperature δT_b due to 21cm emission:

$$P_{\Delta T}(\boldsymbol{k}) = \bar{T}_{\rm sig}^2 P_{\rm obs}(\boldsymbol{k}),$$

$$\bar{T}_{\rm sig} = 190 \frac{x_{\rm H\,I}(z)\,\Omega_{\rm H,0}\,h\,(1+z)^2}{H(z)\,/\,H_0}\,{\rm mK},$$

* The HI bias model:

$$b_i^{\rm H\,I}(z) = \frac{\int_{M_{\rm min}}^{M_{\rm max}} dM\, n(M,z)\, M_{\rm H\,I}(M)\, b_i(M,z)}{\rho_{\rm H\,I}},$$

(Gong et al. 2011)

Generalized Noise Power Spectrum

* The correlation function of the visibilities measured at the discrete baselines u_i and u_j
* The ***noise covariance matrix for visibilities*** (McQuinn et al. 2006; Bharadwaj & Pandey 2003)

$$\mathbf{C}^N(\boldsymbol{u}_i, \boldsymbol{u}_j) = \langle \boldsymbol{\Delta T}_N(\boldsymbol{u}_i) \boldsymbol{\Delta T}^*_{\mathbf{N}}(\boldsymbol{u}_j) \rangle = \left(\frac{\lambda^2 \boldsymbol{T}_{\rm sys} \boldsymbol{\Delta} \nu}{\boldsymbol{A}_{\mathbf{e}}} \right)^2 \frac{\delta_{\mathbf{ij}}}{\boldsymbol{\Delta} \nu \, \boldsymbol{t}_{\boldsymbol{u}}}.$$

* The ***sample variance*** contribution to the covariance matrix is (McQuinn et al. 2006)

$$\begin{aligned}
\mathbf{C}^{\rm SV}(\boldsymbol{u}_i, \boldsymbol{u}_j) &= \langle \delta T_b(\boldsymbol{u}_i) \delta T_b^*(\boldsymbol{u}_j) \rangle \\
&\approx \delta_{ij} \int d^3\boldsymbol{u} |R(\boldsymbol{u}_i - \boldsymbol{u})|^2 P_{\Delta T}(\boldsymbol{u}) \\
&\approx \delta_{ij} \frac{\lambda^2 \Delta\nu^2}{r_a^2(z) \Delta r(z) A_e} P_{\Delta T}(\boldsymbol{k}_{i\perp}, k_{i\parallel}),
\end{aligned}$$

Generalized Noise Power Spectrum

* The total covariance matrix $\mathbf{C} = \mathbf{C}^N + \mathbf{C}^{\mathrm{SV}}$

* Uncertainty of bandpower from the Fisher matrix:

$$F_{ab} = \mathrm{Tr}\left[\mathbf{C}^{-1}\frac{\partial \mathbf{C}}{\partial \boldsymbol{p}_{\mathbf{a}}}\mathbf{C}^{-1}\frac{\partial \mathbf{C}}{\partial \boldsymbol{p}_{\mathbf{b}}}\right]$$

➔ the measurement error:

$$\begin{aligned}\delta P_{\Delta T}(\boldsymbol{k}_i) &= \frac{1}{\sqrt{N_c(\boldsymbol{k}_i)}}\frac{A_e r_a^2 \Delta r}{\lambda^2 \Delta \nu^2}\left[C^N(\boldsymbol{k}_i,\boldsymbol{k}_i) + C^{\mathrm{SV}}(\boldsymbol{k}_i,\boldsymbol{k}_i)\right] \\ &= \frac{1}{\sqrt{N_c(\boldsymbol{k}_i)}}\left[P^N(\boldsymbol{k}_i) + P^{\mathrm{SV}}(\boldsymbol{k}_i)\right], \qquad (25)\end{aligned}$$

* The noise power spectrum:

$$P^N(k,z) = \frac{4\pi f_{\mathrm{sky}}\lambda^2 T_{\mathrm{sys}}^2\, y(z)\, r_a(z)^2}{A_e\, \Omega_{\mathrm{FOV}}\, t_{\mathrm{tot}}}\left(\frac{\lambda^2}{A_e\, n(\boldsymbol{k}_\perp)}\right)$$

Baseline distribution

Tianlai Noise Power Spectra

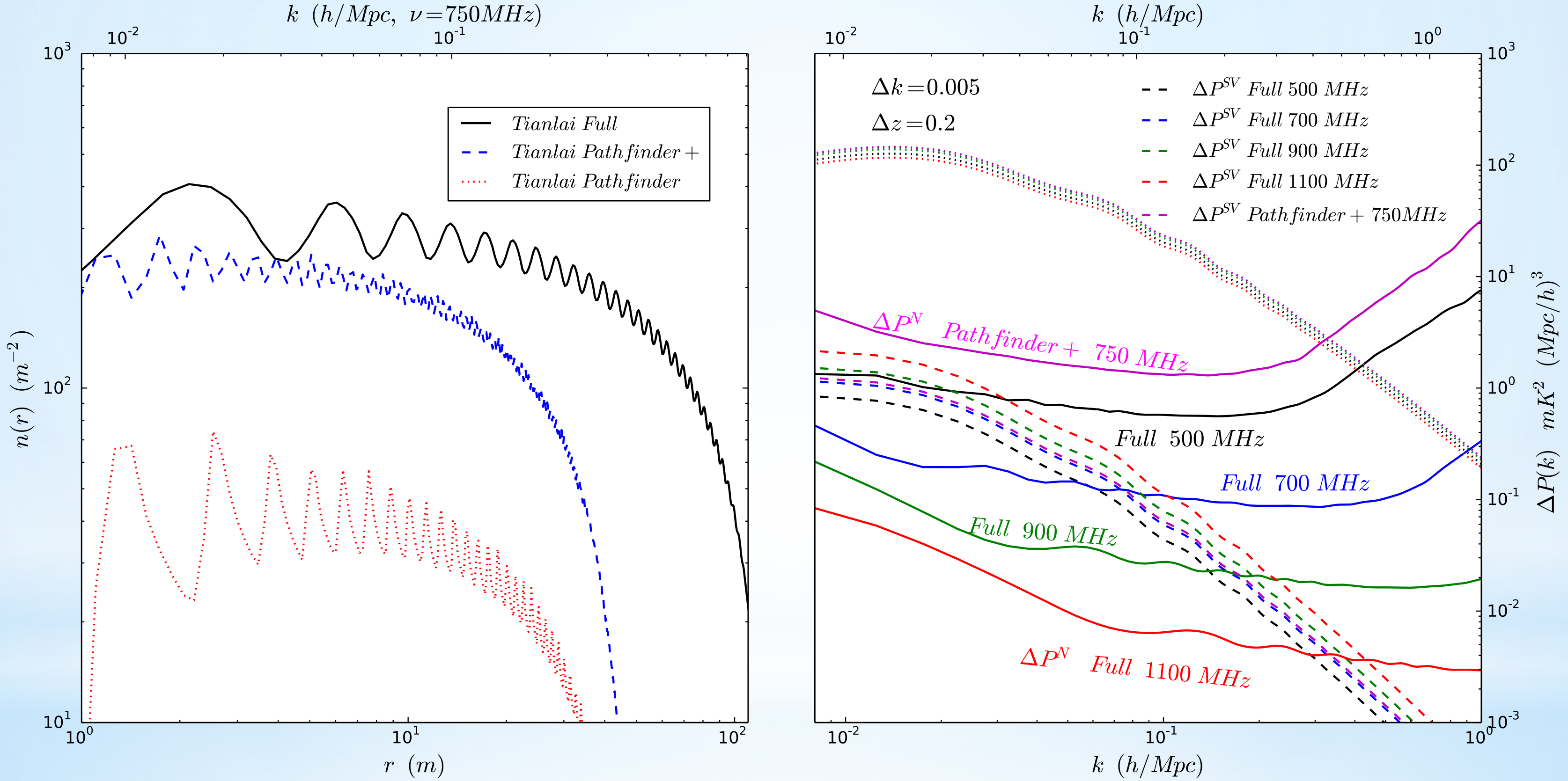

The Power Spectrum with Expected Tianlai Errors

* $$\Delta P_{\rm obs}(\boldsymbol{k}) \;=\; \frac{1}{\sqrt{N_c}}\,\left[P_{\rm obs}(\boldsymbol{k}) + N(k)\right],$$

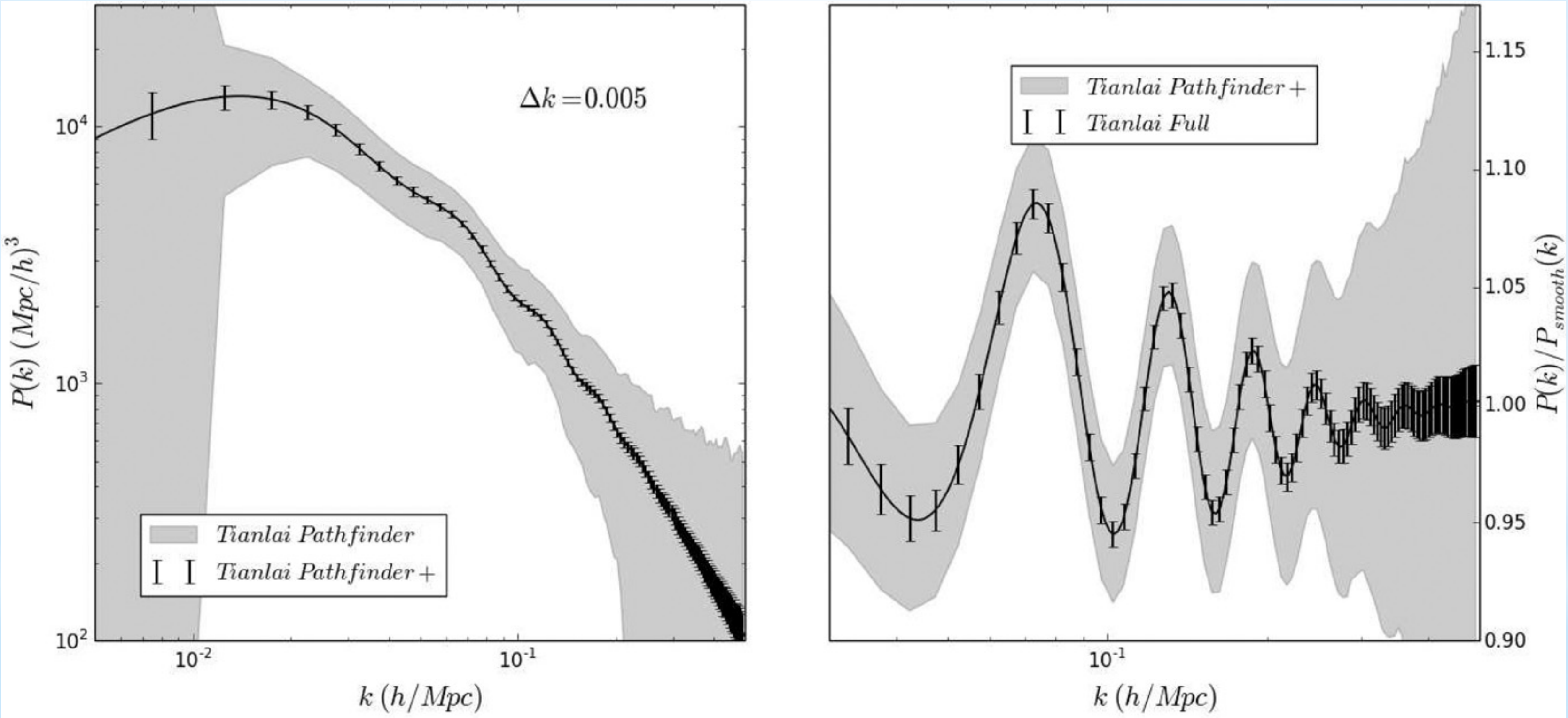

survey area: 10,000 deg^2, integration time: 1 year.

The Fisher Information Matrix

* To predict how well the experiment will be able to constrain the model parameters, ***before doing the experiment***.

* Model $f(p_i)$ + measurement uncertainties (***experimental design***)

↓

Fisher matrix $$\mathcal{F}_{ij} = \sum_b \frac{1}{\sigma_b^2} \frac{\partial f_b}{\partial p_i} \frac{\partial f_b}{\partial p_j}$$

observables

parameters

measurement uncertainties

inverse ↓

covariance matrix
(uncertainties on model parameters)

* The Cramer-Rao limit: $\Delta p_i \geq \left(\mathbf{F}^{-1}\right)_{ii}^{1/2}$

Fisher Forecast on the Constraint on Dark Energy

* From the power spectrum measurement at a given redshift, the Fisher information matrix: (Tegmark 1997; Seo & Eisenstein 2003; Mao et al. 2008)

$$F_{\alpha\beta} = \sum_k \left[\frac{\partial P_{\rm obs}(\boldsymbol{k})}{\partial \alpha} \frac{\partial P_{\rm obs}(\boldsymbol{k})}{\partial \beta} \right] / \left[\Delta P_{\rm obs}(\boldsymbol{k})\right]^2$$

Free parameters α and β: $\{D_{\rm A}(z_i), H(z_i), b_{1,i}^{\rm H\,I}, f(z_i), \text{ and } P_{\rm shot,i}\}$

Nuisance parameters: $\{b_{1,i}^{\rm H\,I}, P_{\rm shot,i}\}$

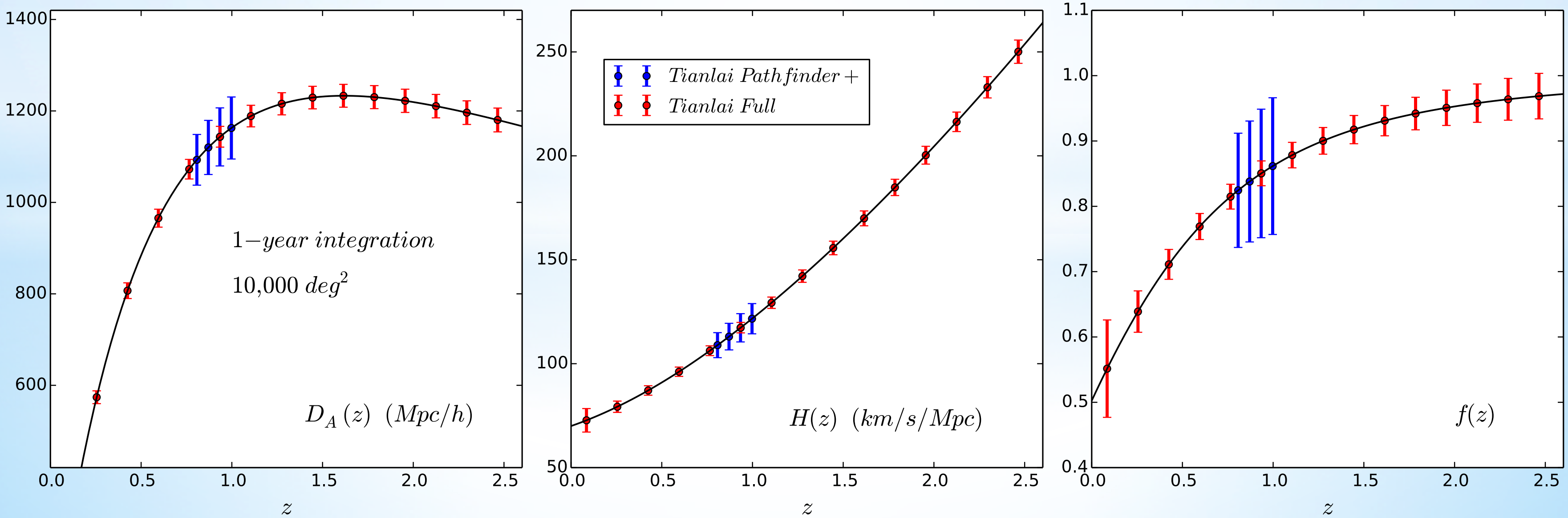

Fisher Forecast on the Constraint on Dark Energy

* DE parameterization: $$w(z) = w_0 + w_a[1 - a(z)] = w_0 + w_a \frac{z}{1+z}.$$
* Converting the parameter space: $$F^{DE}_{mn} = \sum_{\alpha,\beta} \frac{\partial p_\alpha}{\partial q_m} F^{dis}_{\alpha\beta} \frac{\partial p_\beta}{\partial q_n}.$$
* Combine with CMB observations (Wang et al. 2009): $$F^{\rm tot}_{\alpha\beta} = F^{\rm CMB}_{\alpha\beta} + \sum_i F^{\rm IM}_{\alpha\beta}(z_i),$$

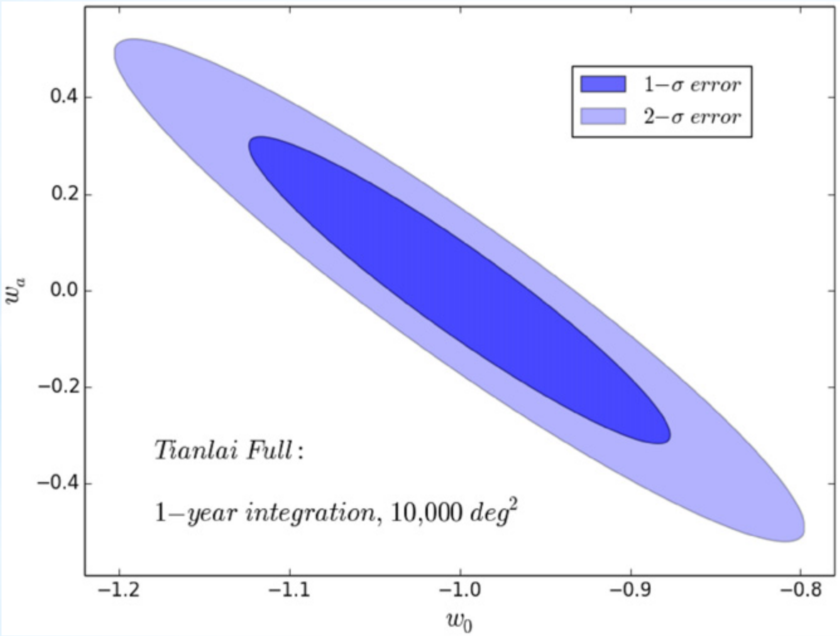

$\sigma_{w0} \approx 0.0815$
$\sigma_{wa} \approx 0.210$

Fisher Forecasts for the PNG

* HI -- a less biased tracer of the underlying matter density

(1) A scale-dependent and redshift-dependent HI bias

  * Most prominent on very large scale – suitable for intensity mapping
  * Camera et al. (2013): a small but compact array working at ~ 400 MHz could possibly achieve $\sigma_{fNL} \sim 1$.

(2) Bispectrum of HI gas distribution

  * The relative importance of primordial non-Gaussianity increases toward higher redshifts

Constraints on f_{NL} from the HI Power Spectrum

* For the standard local type PNG, the scale-dependent non-Gaussian correction to the linear halo bias:

$$\Delta b^d(k, z) = \frac{2\, f_{\rm NL}\, (b_1^{\rm G} - 1)\, \delta_c}{\mathcal{M}(k, z)}$$

halo bias

* The HI bias factors: $b_i^{\rm HI}(z) = \frac{\int_{M_{\min}}^{M_{\max}} dM\, n(M, z)\, M_{\rm HI}(M)\, b_i(M, z)}{\rho_{\rm HI}}$

* The observed HI power spectrum:

$$P_{\rm s}(k, z) = a_0^{\rm P}(\beta)\, P_{\rm H\,I}(k, z),$$

where $P_{\rm HI}(k, z) = \left[b_1^{\rm HI}(k, z)\right]^2 P_{\rm L}(k, z)$

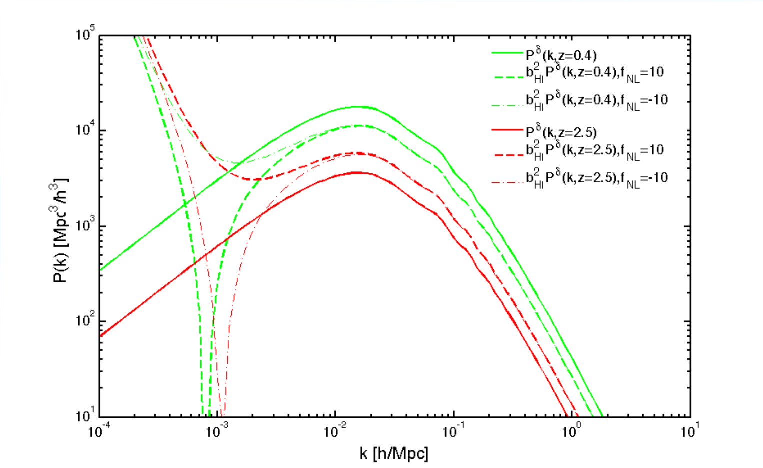

Constraints on f_{NL} from the HI Power Spectrum

* The Fisher information matrix for f_{NL}:

$$F_{\alpha\beta} = \sum_k \left[\frac{\partial P_{\rm obs}(\boldsymbol{k})}{\partial \alpha} \frac{\partial P_{\rm obs}(\boldsymbol{k})}{\partial \beta} \right] / \, [\Delta P_{\rm obs}(\boldsymbol{k})]^2$$

$$\Delta P_{\rm obs}(\boldsymbol{k}) = \frac{1}{\sqrt{N_c}} \, [P_{\rm obs}(\boldsymbol{k}) + N(k)]$$

Table 2

The Predicted 1σ Errors of $f_{\rm NL}$ Using the H I Ppower Spectrum Measured by Tianlai

	Pathfinder	Pathfinder+	Full Scale
$N_{\rm feed}$ per cylinder	32	72	256
$\sigma_{\rm f_{NL}}^{\rm local}$	1504	161	14.1

survey area = 10000 deg^2, integration time = 1 year.

Constraints on f_{NL} from the HI Bispectrum

* The tree-level expression for the reduced HI bispectrum in redshift space after averaging over angles in k space:

$$Q_s(k_1,k_2,k_3) = \frac{a_0^{\rm B}(\beta)}{\left[a_0^{\rm P}(\beta)\right]^2}\left[\frac{1}{b_1^{\rm HI}}\,Q^{\rm tree}(k_1,k_2,k_3) + \frac{b_2^{\rm HI}}{(b_1^{\rm HI})^2}\right]$$

3 - non-linear bias

* The reduced matter bispectrum

2 - non-linear gravitational evolution

$$\begin{aligned} Q^{\rm tree}(k_1,k_2,k_3) &= Q_{\rm I}(k_1,k_2,k_3) + Q_{\rm G}(k_1,k_2,k_3) \\ &= \frac{B_{\rm I}(k_1,k_2,k_3)}{P_{\rm L}(k_1)\,P_{\rm L}(k_2) + (2\,perm.)} + \frac{B_{\rm G}(k_1,k_2,k_3)}{P_{\rm L}(k_1)\,P_{\rm L}(k_2) + (2\,perm.)} \end{aligned}$$

1 - primordial non-Gaussianity

$$B_{\rm I}(k_1,k_2,k_3) = \mathcal{M}(k_1;z)\,\mathcal{M}(k_2;z)\,\mathcal{M}(k_3;z)\,B_\Phi(k_1,k_2,k_3)$$

- Local model
- Equilateral model
- ......

Constraints on f_{NL} from the HI Bispectrum

* The Fisher matrix for observations of reduced bispectrum at a given redshift bin:

$$F_{\alpha\beta} \equiv \sum_{k_1=k_{\min}}^{k_{\max}} \sum_{k_2=k_{\min}}^{k_1} \sum_{k_3=k^*_{\min}}^{k_2} \frac{\partial Q_s}{\partial \alpha} \frac{\partial Q_s}{\partial \beta} \frac{1}{\Delta Q_s^2},$$

* The variance of the reduced HI bispectrum in redshift space:

$$\Delta Q_s^2(k_1, k_2, k_3) \simeq \frac{\Delta B_s^2(k_1, k_2, k_3)}{[P_s(k_1)P_s(k_2) + (2\ perm.)]^2}$$

(Sefusatti & Komatsu 2007)

$$\Delta B_s^2(k_1, k_2, k_3) \simeq (2\pi)^3 V_f \frac{s_{123}}{V_B} P_{\rm tot}(k_1)\, P_{\rm tot}(k_2)\, P_{\rm tot}(k_3),$$

(Scoccimarro et al. 1998)

The total measured power spectrum = $P_{\rm obs}(\boldsymbol{k}) + N(k)$

Noise power spectrum

Constraints on f_{NL} from the HI Bispectrum

* The PNG from ***Tianlai*** intensity mapping

Table 3
The Marginalized 1σ Errors of $f_{\rm NL}$ Using the H I Bispectrum Measured by Tianlai

	Pathfinder	Pathfinder+	Full Scale
$N_{\rm feed}$ per cylinder	32	72	256
$\sigma_{f_{\rm NL}}^{\rm local}$	70814	2272	21.7
$\sigma_{f_{\rm NL}}^{\rm equil}$	79427	2754	157

survey area = 10000 $\rm deg^2$,
integration time = 1 year,
system temperature = 50 K.

400 – 1420 MHz

* The PNG from ***SKA*** intensity mapping
  * SKA1-mid (auto-correlation)

$$\sigma(f_{\rm NL}^{\rm loc}) = 45.7 \text{ and } \sigma(f_{\rm NL}^{\rm eq}) = 214.3$$

  * SKA2-mid (interferometry)

$$\sigma(f_{\rm NL}^{\rm loc}) = 6.6 \text{ and } \sigma(f_{\rm NL}^{\rm eq}) = 55.4$$

survey area = 20000 $\rm deg^2$,
integration time = 5000 hr,
system temperature = 25 K,
350 – 1420 MHz

Summary

* The Tianlai experiment – a cylinder array to map the large-scale structure of matter distribution
* Assuming t_{int} ~ 1 year and a survey area of 10,000 deg^2, we expect $\sigma_{w0} \sim 0.082$ and $\sigma_{wa} \sim 0.21$ from the BAO and RSD measurements. (This is comparable to stage IV dark energy experiments, while the cost would only be a small fraction of such experiments.)
* To constrain PNG, we find $\sigma_{fNL}^{local} \sim 14$ from the power spectrum measurements with scale-dependent bias, and $\sigma_{fNL}^{local} \sim 22$ and $\sigma_{fNL}^{equil} \sim 157$ from the bispectrum measurements.

THANK YOU!

Generalized Noise Power Spectrum

* The visibility:

$$V_{\alpha\beta,[\mathrm{Jy}]}(\boldsymbol{u}_{\alpha\beta},\nu) = \int d^2\hat{n} e^{-i2\pi\hat{n}\cdot\boldsymbol{u}_{\alpha\beta}} A_\alpha(\hat{n},\nu)A^*_\beta(\hat{n},\nu)I(\hat{n},\nu)$$

$$\approx \int d^2\hat{n} e^{-i2\pi\hat{n}\cdot\boldsymbol{u}_{\perp}} A_\alpha(\hat{n},\nu)A^*_\beta(\hat{n},\nu)I(\hat{n},\nu),$$

Rayleigh-Jeans approximation

$$V_{\alpha\beta,[\mathrm{K}]}(\boldsymbol{u}_{\perp},\nu) = \int d^2\hat{n} e^{-i2\pi\hat{n}\cdot\boldsymbol{u}_{\perp}} A_\alpha(\hat{n},\nu)A^*_\beta(\hat{n},\nu)\delta T_b(\hat{n},\nu).$$

FT w.r.t. ν

$$V_{\alpha\beta,[\mathrm{K\cdot MHz}]}(\boldsymbol{u}_{\perp},u_{\parallel}) = \int d\nu e^{-i2\pi\nu u_{\parallel}} V_{\alpha\beta,[\mathrm{K}]}(\boldsymbol{u}_{\perp},\nu).$$

* The thermal noise:

$$\delta V_{\alpha\beta,[\mathrm{K}]}(\boldsymbol{u}_{\perp},\nu) = \frac{\lambda^2 T_{\mathrm{sys}}}{A_e\sqrt{\Delta\nu t_{\boldsymbol{u}}}},$$

T_{sys}= 50 K

$$\Delta T_N(\boldsymbol{u}) = \frac{T_{\mathrm{sys}}}{\sqrt{\Delta\nu t_{\boldsymbol{u}}}}\left(\frac{\lambda^2\Delta\nu}{A_e}\right).$$

$$\boldsymbol{u} \equiv \{\boldsymbol{u}_{\perp}, u_{\parallel}\} \quad \xleftrightarrow{\text{FT}} \quad \boldsymbol{\theta} = \{\hat{n},\nu\}$$